iScience, Volume *24*

Supplemental information

Myofiber androgen receptor increases muscle strength mediated by a skeletal muscle splicing variant of Mylk4

Iori Sakakibara, Yuta Yanagihara, Koichi Himori, Takashi Yamada, Hiroshi Sakai, Yuichiro Sawada, Hirotaka Takahashi, Noritaka Saeki, Hiroyuki Hirakawa, Atsushi Yokoyama, Soichiro Fukada, Tatsuya Sawasaki, and Yuuki Imai

Figure S1

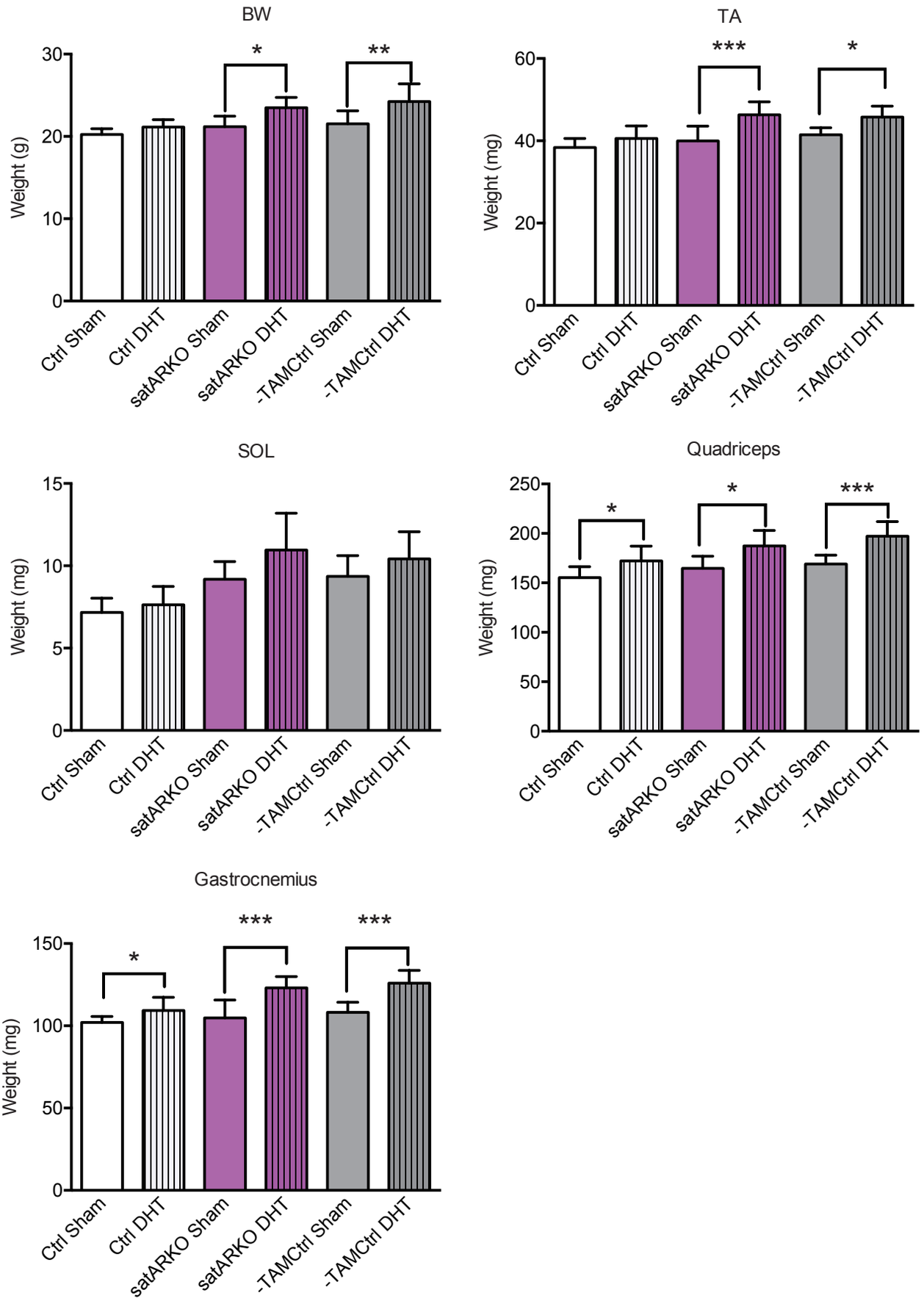
BW
Weight (g)
30
20
10
0
*
**
Ctrl Sham
Ctrl DHT
satARKO Sham
satARKO DHT
-TAMCtrl Sham
-TAMCtrl DHT
TA
Weight (mg)
60
40
20
0
***
*
SOL
Weight (mg)
15
10
5
0
Quadriceps
Weight (mg)
250
200
150
100
50
0
*
*
***
Gastrocnemius
Weight (mg)
150
100
50
0
*
***
***

Figure S2

A

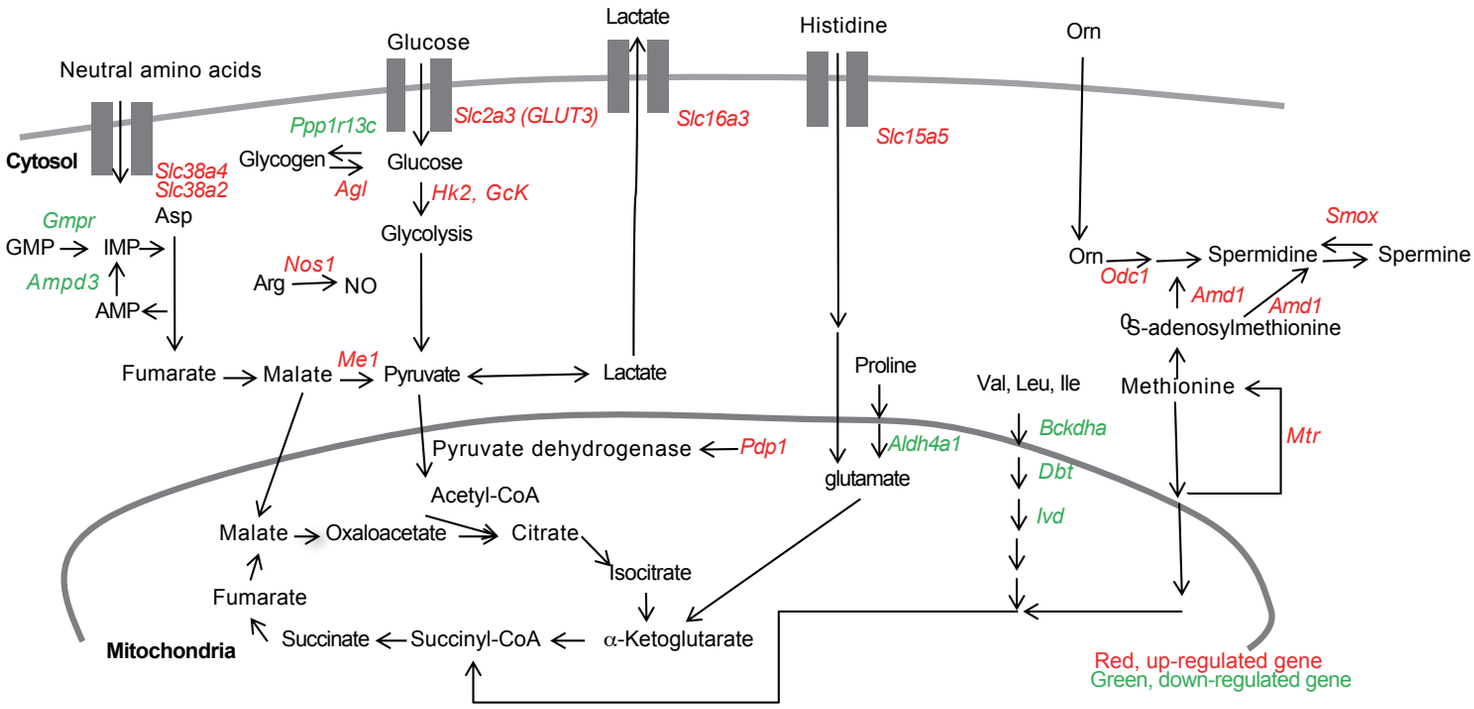

B

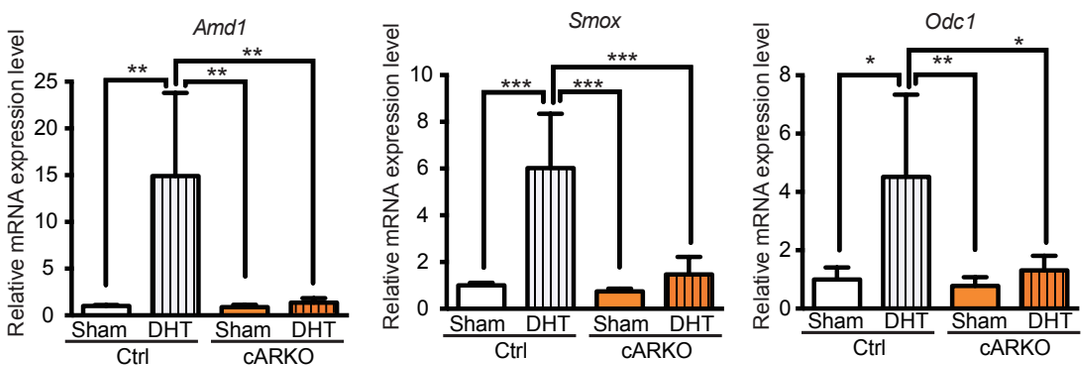

C

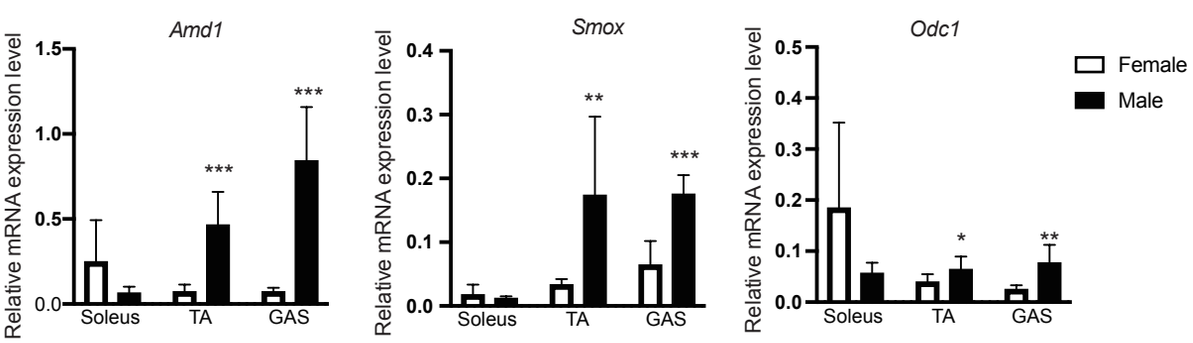

Figure S3

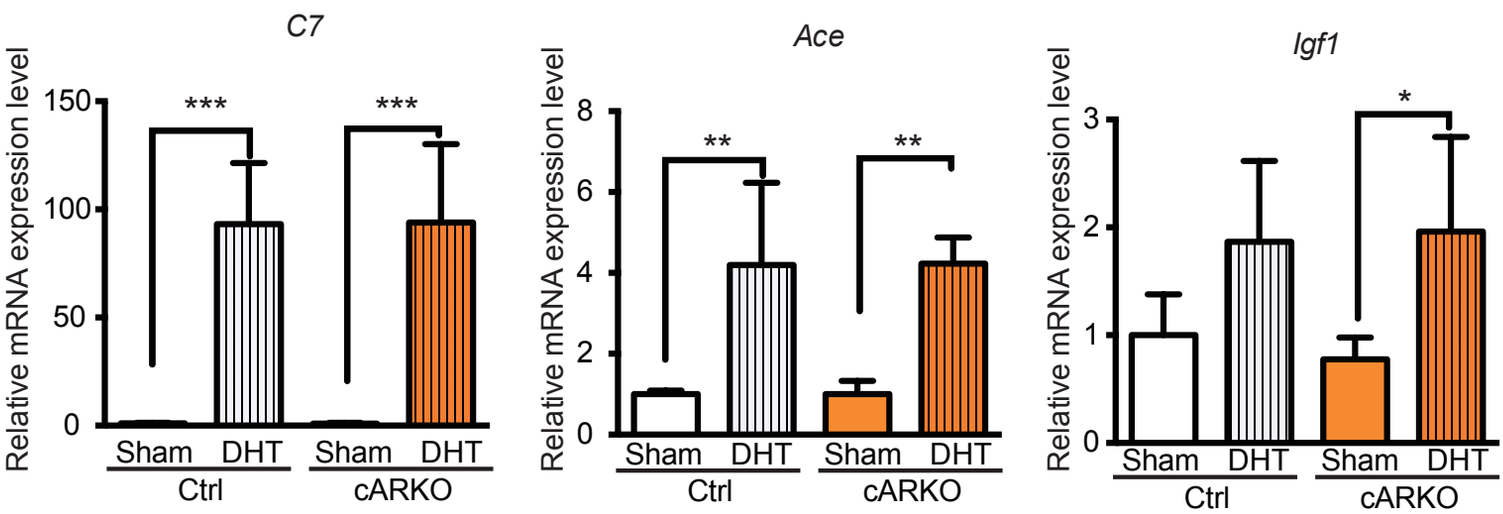
C7
Relative mRNA expression level
150
100
50
0
***
***
Sham
DHT
Sham
DHT
Ctrl
cARKO
Ace
Relative mRNA expression level
8
6
4
2
0
**
**
Sham
DHT
Sham
DHT
Ctrl
cARKO
Igf1
Relative mRNA expression level
3
2
1
0
*
Sham
DHT
Sham
DHT
Ctrl
cARKO

Figure S4

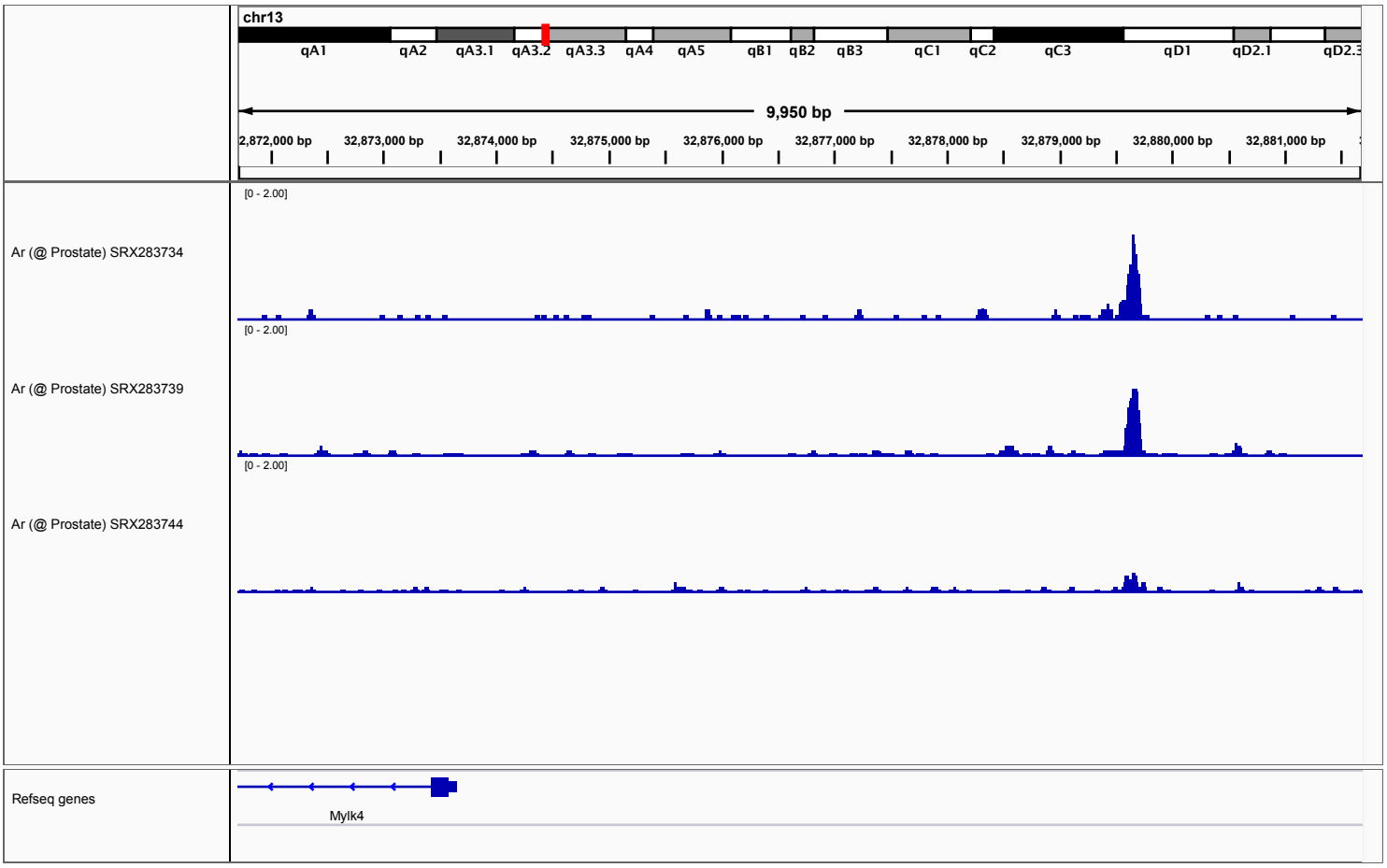
chr13
qA1
qA2
qA3.1
qA3.2
qA3.3
qA4
qA5
qB1
qB2
qB3
qC1
qC2
qC3
qD1
qD2.1
9,950 bp
32,872,000 bp
32,873,000 bp
32,874,000 bp
32,875,000 bp
32,876,000 bp
32,877,000 bp
32,878,000 bp
32,879,000 bp
32,880,000 bp
32,881,000 bp
[0 - 2.00]
Ar (@ Prostate) SRX283734
[0 - 2.00]
Ar (@ Prostate) SRX283739
[0 - 2.00]
Ar (@ Prostate) SRX283744
Refseq genes
Mylk4

Figure S5


MYLK2 ----MTTENGAVELGSQSLSTEQTPKAAAGDGPSASEKEPSAPATEKDLSPPNAKKDPGAPDPKNNPDPPSLKKDPAKAPGPEKKGDPVPASASSQGPSGEGDGGGGPAEGSEGPPAALP
cMYLK4 ----------MLKVKRLEEISSCHSSNPLEKVAFFQCMEEVEKVKCFLEENSGDLDLQSGDNEAEENVWSNRALDERIIVKGGRTSA
skmMYLK4 MSSYRCQEKGVLSSHDCVLIYKSETEGDESPTPDSSLIRLTTSMLKVKRLEEISSCHSSNPLEKVAFFQCMEEVEKVKCFLEENSGDLDLQSGDNEAEENVWSNRALDERIIVKGGRTSA
MYLK2 LPTATAEASIQKLDPTQAPSGNQGSGEAKAG----------KKAAECRE
cMYLK4 LTD----------
skmMYLK4 LTEKTDQNDQFSSEKEKITKLNKKNSEKTSALEVQRSCVICHVERQDKIEFVQRNSTELRENAGAKDAPCIESLEKQESNNLRDKQDTEDNNGGENGISSKDDSRGVEAENRASAAASGA
MYLK2 AGRRGSPAFLHSPSCPAIISCSEKTLAVKPLSETTDLVFTGVSVTPDPQDPGPVKAGGTNALAEKKKEEAEKASGQAGQAKVQGDTPQRIGFQAVPSERVEVGQALCLTAREEDCFQILD
cMYLK4 ----------
skmMYLK4 VLDKHSTESQHTEDMNGDPSHERCISNIKTTSTPGILGNSASGSTFQNAEQTESTGSSKRRVAEECFLSEDNKKSRIDVVRRGEEPTARTEETRQARSLGDRLQDGMTTSREQDLEVPLD
MYLK2 DCPPPPAPFPHRIVELRTGNVNSEFSMNSKEALGGGKFGAVCTCTERATGLKLAAKVIKKQTPKDKEMVLLEIEVMNQLNHRNLIQLYAAIETSHEIILFMEYIEGGELFERIVDEDYHL
cMYLK4 DIPAPAAPFDHRMVMAKHASVDNLYTVSKSEILGGGRFGQVHKCEEKATGLKLAAKIIKTRGAKDKEDVKNEISVMNQLDHVNLIQLYDAFESKHDIILVMEYVEGGELFDRIIDENCNL
skmMYLK4 DIPAPAAPFDHRMVMAKHASVDNLYTVSKSEILGGGRFGQVHKCEEKATGLKLAAKIIKTRGAKDKEDVKNEISVMNQLDHVNLIQLYDAFESKHDIILVMEYVEGGELFDRIIDENCNL
MYLK2 TEVDTMVFVRQICDGILFMHKMRVLHLDLKPENILCVNTTGHLVKIIDFGLARRYNPNEKLKVNFGTPEFLSPEVVNYDQISDKTDMWSLGVITYMLLSGLSPFLGDDDTETLNNVLSAN
cMYLK4 TELDTILFMKQICEGIRYMHQMYILHLDLKPENILCVNRTAKQIKIIDFGLARRYKPREKLKVNFGTPEFLAPEVVNYDFVSFSTDMWSVGVITYMLLSGLSPFLGDNDAETLTNILACR
skmMYLK4 TELDTILFMKQICEGIRYMHQMYILHLDLKPENILCVNRDAKQIKIIDFGLARRYKPREKLKVNFGTPEFLAPEVVNYDFVSFSTDMWSVGVITYMLLSGLSPFLGDNDAETLTNILACR
MYLK2 WYFDEETFEAVSDEAKDFVSNLLTKDQSARMSAEQCLAHPWLNNLAEKAKRCNRRLKSQILLKKYLMKRRWKKNFIAVSAANRFKKISSSGALMALGV
cMYLK4 WDLEDEEFQDISEEAKEFISKLLIKEKSWRISASEALKHPWLSDHKLHSRLSAQKNCNSGVLNLTTK----------
skmMYLK4 WDLEDEEFQDISEEAKEFISKLLIKEKSWRISASEALKHPWLSDHKLHSRLSAQKNCNSGVLNLTTK----------

Figure S6

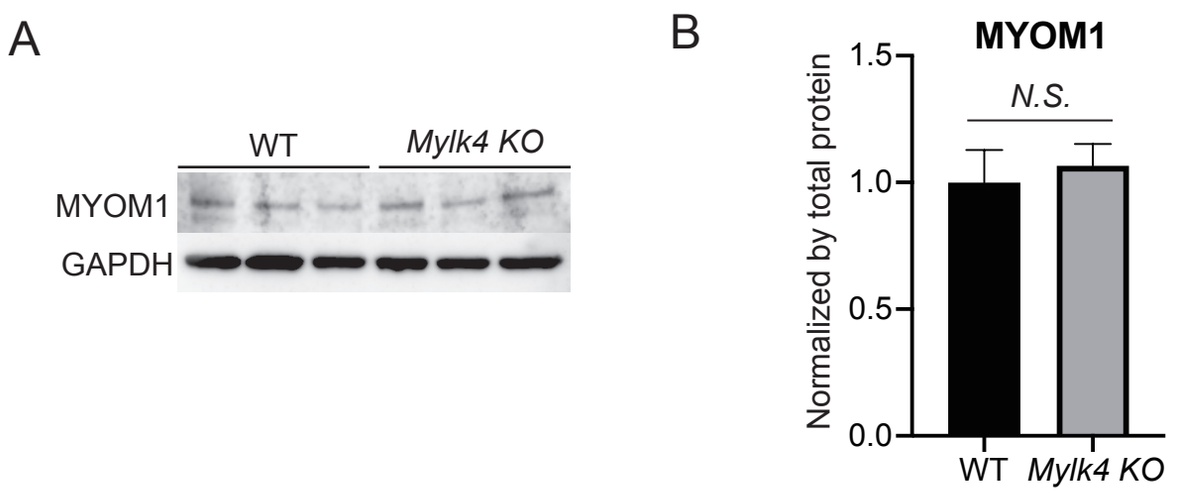
A
WT
Mylk4 KO
MYOM1
GAPDH
B
MYOM1
N.S.
Normalized by total protein
1.5
1.0
0.5
0.0
WT
Mylk4 KO

Figure S7

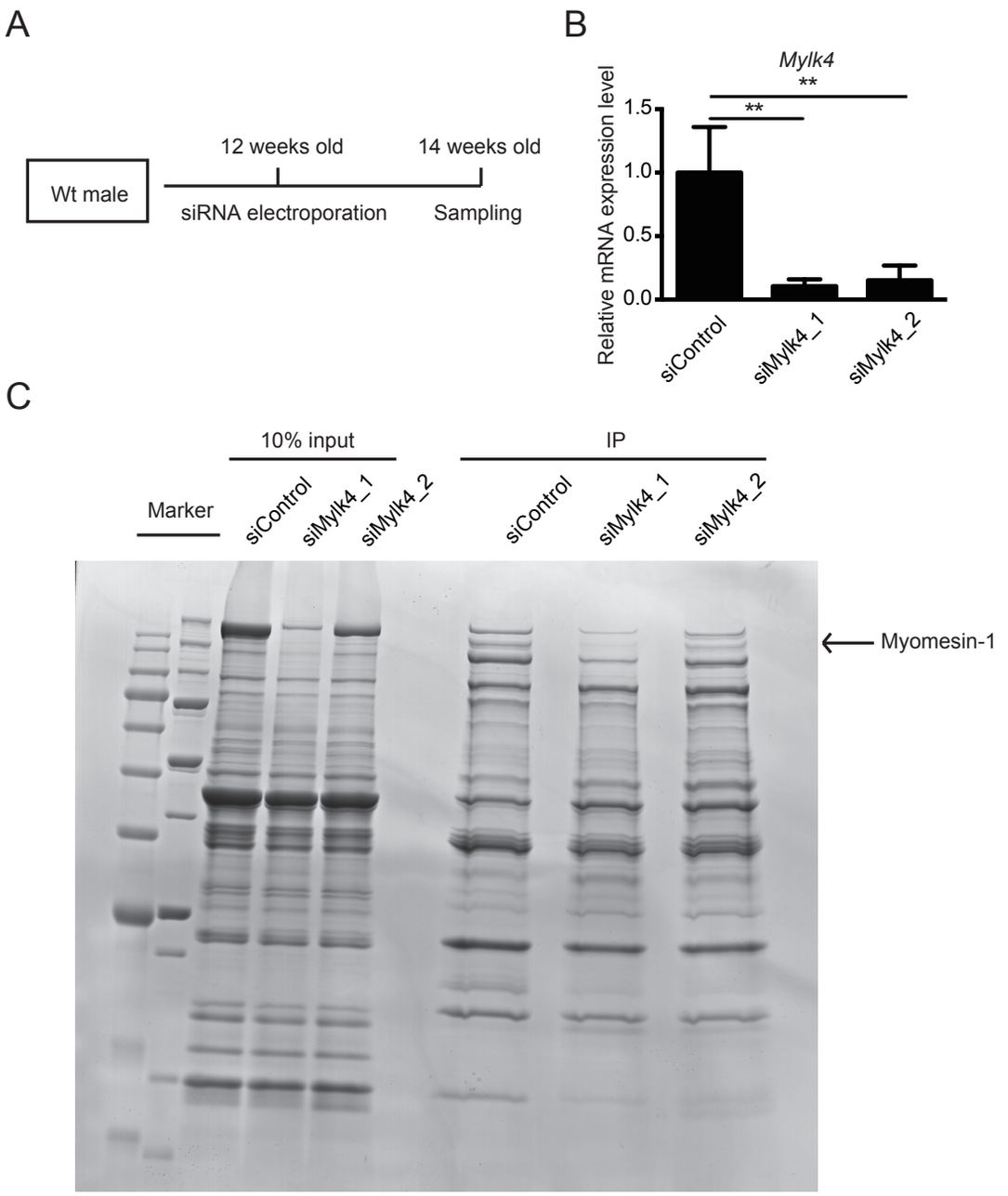
A
12 weeks old
14 weeks old
Wt male
siRNA electroporation
Sampling
B
Mylk4
**
**
Relative mRNA expression level
1.5
1.0
0.5
0.0
siControl
siMylk4_1
siMylk4_2
C
10% input
IP
Marker
siControl
siMylk4_1
siMylk4_2
siControl
siMylk4_1
siMylk4_2
Myomesin-1

Figure S8

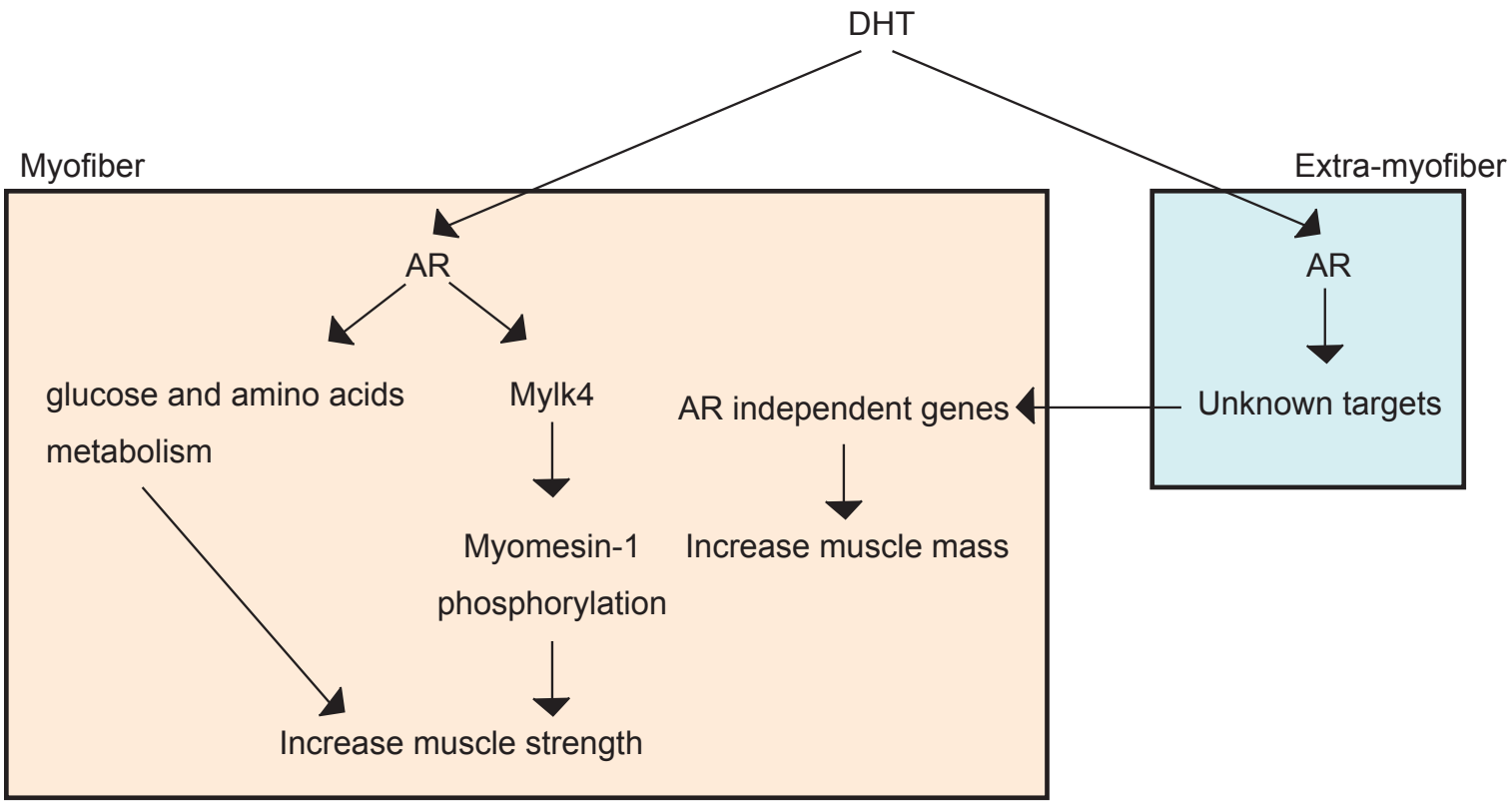
DHT
Myofiber
Extra-myofiber
AR
AR
glucose and amino acids
metabolism
Mylk4
AR independent genes
Unknown targets
Myomesin-1
phosphorylation
Increase muscle mass
Increase muscle strength

Supplemental information

Figure S1. *Ar* deletion in a satellite cell did not affect DHT-induced muscle hypertrophy, Related to Figure 1. Nine-week-old female control and *satARKO* mice were implanted with a pellet containing 10 mg DHT. Body weight, TA muscle weight, soleus muscle (SOL) weight, quadriceps muscle weight, and gastrocnemius muscle weight were measured in 13-week-old female Ctrl_Sham (n=7), Ctrl_DHT (n=6), satARKO_Sham (n=5), satARKO_DHT (n=5), -TAMCtrl_Sham (n=6), and -TAMCtrl_DHT (n=6) mice. Data are represented as mean ± SD. *P<0.05, **P<0.01, ***P<0.001. One-way ANOVA followed by Student Newman-Keuls tests.

Figure S2. Enhanced glucose utilization and suppressed amino acid catabolism by AR, Related to Figure 2. (*A*) Genes coding for the glycolytic pathway and amino acid metabolism are represented. Genes whose expression is modified in *cARKO* are indicated as red (up) or green (down). (*B*) mRNA expression levels of *Amd1*, *Smox and Odc1* in gastrocnemius muscles of 13-week-old female Control_Sham (n=4), Control_DHT (n=3), cARKO_Sham (n=4), and cARKO_DHT (n=5) mice. *P<0.05, **P<0.01, ***P<0.001. (*C*) *Amd1*, *Smox and Odc1* gene expression was determined in soleus muscles, TA muscles, and gastrocnemius muscles of male or female mice by RT-qPCR (n=8, each tissue). Data are represented as mean ± SD. *P<0.05, **P<0.01, ***P<0.001. One-way ANOVA followed by Student Newman-Keuls tests.

Figure S3. mRNA expression levels of *C7*, *Ace and Igf1*, Related to Figure 2. mRNA expression levels of *C7*, *Ace and Igf1* in gastrocnemius muscles of 13-week-old female Control_Sham (n=4), Control_DHT (n=3), cARKO_Sham (n=4), and cARKO_DHT (n=5) mice. Data are represented as mean ± SD. *P<0.05, **P<0.01, ***P<0.001. One-way ANOVA followed by Student Newman-Keuls tests.

Figure S4. AR binding at the *Mylk4* gene locus, Related to Figure 3. Genome viewer for registered ChIP-seq against AR (GSE47119) at the *Mylk4* gene locus in mouse prostates.

Figure S5. Alignment of amino acid sequence of MYLK2, cardiac MYLK4 (cMYLK4) and skeletal muscle MYLK4 (skmMYLK4), Related to Figure 3. '*' indicates positions which have a single, fully conserved residue; ':' indicates that one of the following 'strong' groups is fully conserved: STA, NEQK, NHQK, NDEQ, QHRK, MILV, MILF, HY, FYW; '.' indicates that one of

the following 'weaker' groups is fully conserved: CSA, ATV, SAG, STNK, STPA, SGND, SNDEQK, NDEQHK, NEQHRK, FVLIM, HFY. Amino acid sequence of MYLK2 underlined with red, green and blue indicate kinase domain, autoinhibitory regulatory segment and CaM binding regulatory segment, respectively.

Figure S6. MYOM1 protein levels in Mylk4 KO mice is comparable with WT mice, Related to Figure 4.

(*A*) Western blot analyses for MYOM1 using total lysates of quadriceps muscles obtained from WT and *Mylk4 KO* mice. GAPDH was used as a loading control. (*B*) Quantitative analysis of western blot. The signal of MYOM1 from the immunoblot analyses were normalized to the total protein concentration of each samples and WT signals (n=3). *N.S.* indicates not significant. Two-tailed, unpaired Student's *t* tests.

Figure S7. MYOM1 phosphorylation is decreased by knockdown of *Mylk4*, Related to Figure 4. (*A*) An experimental scheme. TA muscles of 12-week-old male wild type mice were electroporated with 40 pmol siRNA against *Mylk4*. Two weeks later, TA muscles were analyzed. (*B*) *Mylk4* mRNA expression levels in TA muscles of 14-week-old male siControl (n=3), si*Mylk4*_1 (n=3), and si*Mylk4*_2 (n=3) mice. **P<0.01. (*C*) Phosphorylated proteins were enriched from WT and *Mylk4* knockdown mice and analyzed by SDS-PAGE. Two-tailed, unpaired Student's *t* tests. Data are represented as mean ± SD.

Figure S8. A model of AR controlling muscle strength and muscle mass, Related to Figure 4.

TRANSPARENT METHODS

Materials and Methods

Animals and ethics statement

Protocols of animal experiments were approved by the Animal Experiments Committee of Ehime University and Sapporo Medical University, and were performed in accordance with the Guidelines of Animal Experiments of Ehime University and Sapporo Medical University. *Ar*$^{flox/flox}$*;HSA-Cre* conditional knockout mice (*cARKO*) were obtained by breeding *Ar-LoxP* mice (Kato et al., 2004) and transgenic mice expressing a Cre recombinase under the control of the human skeletal actin promoter (HSA) (Miniou et al., 1999). *Ar*$^{flox/flox}$*;Pax7*$^{CreERT2/+}$ conditional

knockout mice (*satARKO*) were obtained by breeding *Ar-LoxP* mice (Kato et al., 2004) and knock-in mice expressing a Cre^{ERT2} recombinase under the control of the *Pax7* promoter (Lepper et al., 2009). Eight-week-old female *satARKO* mice were given intraperitoneal injection of tamoxifen (1 mg per mouse per day; Sigma) for 5 consecutive days. DHT tablet (SA-161, Innovative Research of America, Sarasota, FL, USA) implantation was performed under isoflurane anesthesia, and all efforts were made to minimize suffering. Each littermate group was divided into the Sham operation group or DHT supplementation group, equally as possible.

Grip strength

Mice forelimb grip strength was measured with a strain gauge (GPM-100B, Melquest, Toyama City, Toyama, Japan). Measurements were repeated ten times, and the maximal force was recorded. The mean value of two records was used as the grip strength of each mouse.

RNA preparation

Gastrocnemius muscles were collected from *cARKO* and control mice. Total RNAs were extracted using ISOGEN Reagent (Nippon Gene, Chiyoda, Tokyo, Japan) and RNeasy Mini Kit (Qiagen, Hilden, Germany) according to the manufacturer's instructions.

cDNA synthesis and qPCR

RNAs were reverse-transcribed with PrimeScript RT Master Mix (RR036A, Takara, Kusatsu, Shiga, Japan) according to the manufacturer's instructions. Reverse transcription was performed with 500 ng of total RNA. Quantitative real time PCR was performed using SYBR Premix Ex Taq II (RR820L, Takara, Kusatsu, Shiga, Japan) according to the manufacturer's protocols. PCR was performed for 40 cycles at 95 °C for 5 seconds and 60 °C for 30 seconds using the Thermal Cycler Dice Real Time System (Takara, Kusatsu, Shiga, Japan). Gene expression levels were normalized by the expression level of the housekeeping gene *Actb*. The sequences of the oligonucleotides used in this study are given in Supplementary Table S1. For PCR analysis of Mylk4, fragments were amplified with forward 5'-GAGATGAAAGCCCCACTCCT -3' and reverse 5'- CTCCAATGCATCCTCCAGAT -3'.

RNA sequencing

Libraries were generated from one μg of total RNA by a TruSeq Stranded mRNA LT Sample Prep Kit (Illumina, San Diego, CA, USA) according to the manufacturer's instructions. 18 pM of

each library was sequenced on Miseq (Illumina) with MiSeq Reagent kit V3 150 cycle (Illumina, San Diego, CA, USA) by 75 base pair end. The reads were mapped on the mouse genome (mm10) by Tophat, and read numbers were counted by FeatureCounts. Differentially expressed genes were determined by an exact test after normalization. RNA sequencing data have been deposited in the Gene Expression Omnibus as accession no. GSE152756. Hierarchical clustering of 529 DEGs was performed by MeV software (Saeed et al., 2003). Pathway analysis was performed by using DAVID Bioinformatics Resources(Huang da et al., 2009a, b).

Immunoblot Analysis

Homogenized tissues were lysed in RIPA buffer (10 mM Tris HCL (pH 7.4); 150 mM NaCl, 5 mM EDTA (pH 7.4); 1% Triton X-100; 1% Sodium deoxycholate; 0.1% sodium dodecyl sulphate) supplemented with protease inhibitor cocktail (Nacalai Tesque, Kyoto, Japan). The immunoblot analysis was performed with tissue lysates of quadriceps muscles using the capillary electrophoresis system (Jess, ProteinSimple). Samples were loaded on the Jess separation module (12 to 230 kDa). The Myomesin 1 peaks were normalized to the total protein concentration using a protein normalization kit (ProteinSimple) and quantified using the Jess quantification module.

Immunohistochemistry

Immunofluorescence staining for AR was performed as previously described (Sakai et al., 2020) with modifications. Briefly, muscles were frozen in liquid nitrogen-chilled isopentane. For immunofluorescence staining, 10 μm cryosections were collected and sections were fixed with 4% paraformaldehyde (PFA) in PBS for 5 min followed by permeabilization with a buffer containing 0.3% Triton X-100 in PBS for 10 min. Slides were washed, blocked with 5% goat serum in PBS and incubated with respective antibodies overnight at 4˚C. The slides were washed and stained with secondary antibodies. Antibodies used for the immunofluorescence were anti-AR (Abcam, Cat# ab105225) and Alexa fluor 488 goat anti-rabbit IgG (Invitrogen, Cat# A-11008).

Electroporation

In vivo transfections were carried out on 12-week-old C57Bl6N mice. For each experimental condition, three to five TA muscles belonging to different mice were used. Under isoflurane anesthesia, legs were shaved and muscles were pre-treated by injection of a sterile 0.9% NaCl

solution containing 0.4U of bovine hyaluronidase/μl two hours before siRNA injection. Four hundred pmol of stealth siRNA (Invitrogen, Carlsbad, CA, USA) and 100 ng of GFP expression plasmid were introduced into TA muscles by electroporation as previously described (Sakakibara et al., 2016). Two weeks following electroporation, mice were euthanized and electroporated muscles were frozen in liquid nitrogen before processing for RNA or protein extraction.

Phosphoprotein proteomics

Phosphoproteins were enriched from TA muscle lysates by a TALON PMAC Magnetic phosphoprotein enrichment kit (635641, Clontech) according to the manufacturer's instructions. The eluate fractions were analyzed by SDS-PAGE, and bands were excised from the gel and analyzed by LC-MS/MS. Briefly, extracted peptides were analyzed by ESI-MS/MS using a Q Exactive Orbitrap instrument (Thermo Fisher Scientific, Pittsburgh, PA, USA). MS spectra were recorded over a range of 350−1500 m/z, followed by data-dependent higher energy collisional dissociation (HCD) MS/MS spectra generated from the ten highest intensity precursor ions. For protein identification, spectra were processed using Proteome Discoverer Version 1.3.0.339 (Thermo Fisher Scientific) against the Mascot algorithm. For database searches, mouse.fasta built from the SwissProt was used. The following parameters were used for the searches: tryptic cleavage, up to two missed cleavage sites, and tolerances of ± 10 ppm for precursor ions, and ± 0.5 Da for MS/MS fragment ions. Mascot searches were performed allowing optional methionine oxidation, serine/threonine phosphorylation and fixed cysteine carbamidomethylation. Proteins that contained peptides with Mascot Significance Threshold > 0.05 were selected.

Generation of *Mylk4* knockout mice

Mylk4 knockout mice were generated by CRISPR/ Cas9-based genome editing delivered by electroporation as previously described (Hashimoto and Takemoto, 2015). The guide RNA sequences were 5'-TTCATCTAGTGCACGGTTGG-3' and 5'-CATCCGATGATCAAATGGAG-3'.

Measurement of *in situ* maximum isometric torque and post-tetanic potentiation

Measurement of *in situ* maximum isometric torque (MIT) and post-tetanic potentiation was described previously (Bowslaugh et al., 2016; Yamada et al., 2019). In short, plantar flexor (PF)

muscles were stimulated supra-maximally (45V, 0.5 ms monophasic rectangular pulse) using a pair of surface electrodes that were placed on the skin. Isometric twitch responses in PF muscles were obtained one min before and 15 s after a potentiating stimulus (PS) consisting of four brief trains of 150 Hz stimulation of 400 ms duration (i.e., MIT) within 10 s (Bowslaugh et al., 2016). Immediately after the measurement, mice were euthanized by cervical dislocation under isoflurane anesthesia and the PF muscles were excised from each animal. Absolute PF torque was normalized to the whole muscle weight for PFs. Post-tetanic potentiation was calculated as the post-PS value divided by the pre-PS value.

Measurement of active and passive force in skinned fibers

The preparation of chemically skinned fiber and the measurement of Ca^{2+}-activated force were described previously (Yamada et al., 2019). A part of the excised TA muscle was pinned out at resting length under paraffin oil and was kept at 4°C. The single muscle fibers were dissected under a stereo-microscope. Four to six skinned fibers were obtained from one whole muscle. A segment of the skinned fiber was connected to a force transducer (Muscle tester, World Precision Instruments) and then incubated with a *N*-2-hydroxyethylpiperazine-*N*'-2-ethanesulfonic acid (HEPES) buffered solution (see below) containing the detergent Triton X-100 (1% (v/v), 10 min treatment) to remove all membranous structures. Fiber length was adjusted to optimal length (2.5 μm) by laser diffraction as described previously (Allen and Kurihara, 1982) and the contractile properties were measured at room temperature (24°C). The solutions used in the skinned fiber analyses were composed of 36 mM Na^+, 126 mM K^+, 90 mM HEPES, 8 mM ATP and 10 mM creatine phosphate, and had a pH of 7.09–7.11 at 24°C (Watanabe and Wada, 2016). The free Mg^{2+} concentration was set at 1.0 mM. The maximum Ca^{2+} solution additionally contained 49.5 mM Ca-EGTA and 0.5 mM free EGTA whereas the relaxation solution contained 50 mM free EGTA. Force-pCa (-log free Ca^{2+} concentration) curves were established with various pCa solutions (pCa 6.4, 6.2, 6.0, 5.8, 5.6, 5.4, and 4.7) prepared by mixing the maximum Ca^{2+} solution and the relaxation solution in appropriate ratios according to the affinity constants reported by Moisescu and Thieleczek (Moisescu and Thieleczek, 1978). The contractile apparatus was directly activated by exposing the skinned fiber to various pCa solutions and the peak force production in each pCa was measured.

The activating solution was then replaced with relaxing solution and the passive force was measured as described previously (Prado et al., 2005). Fibers were stretched from slack sarcomere length (SL, 2.0-2.2 μm) in six steps of ~0.2 μm/sarcomere (complete within 1 s) to a maximum SL, while passive force was recorded during a 2 min pause after each step. Following the last stretch-hold, fibers were released back to slack SL to test for possible shifts of baseline force. From the recordings, we measured the force at the end of each hold period. The cross-sectional area of fibers was calculated from measurements of their diameters. All skinned fibers were used to determine the Ca^{2+}-activated and passive force per cross-sectional area.

Determination of serum DHT

Serum DHT levels were determined by ELISA with a dihydrotestosterone ELISA kit (KA1886, Abnova) according to the manufacturer's instructions.

Statistical analyses

All graphs represent mean values ± SD. Significant differences between mean values were evaluated using two-tailed, unpaired Student's *t* tests (when two groups were analyzed) or one-way ANOVA followed by Student Newman-Keuls tests (for three or more groups).

Supplemental References

Allen, D.G., and Kurihara, S. (1982). The effects of muscle length on intracellular calcium transients in mammalian cardiac muscle. J Physiol *327*, 79-94.

Bowslaugh, J., Gittings, W., and Vandenboom, R. (2016). Myosin light chain phosphorylation is required for peak power output of mouse fast skeletal muscle in vitro. Pflugers Archiv : European journal of physiology *468*, 2007-2016.

Hashimoto, M., and Takemoto, T. (2015). Electroporation enables the efficient mRNA delivery into the mouse zygotes and facilitates CRISPR/Cas9-based genome editing. Sci Rep *5*, 11315.

Huang da, W., Sherman, B.T., and Lempicki, R.A. (2009a). Bioinformatics enrichment tools: paths toward the comprehensive functional analysis of large gene lists. Nucleic acids research *37*, 1-13.

Huang da, W., Sherman, B.T., and Lempicki, R.A. (2009b). Systematic and integrative analysis of large gene lists using DAVID bioinformatics resources. Nat Protoc *4*, 44-57.

Kato, S., Matsumoto, T., Kawano, H., Sato, T., and Takeyama, K. (2004). Function of androgen receptor in gene regulations. The Journal of steroid biochemistry and molecular biology *89-90*, 627-633.

Lepper, C., Conway, S.J., and Fan, C.M. (2009). Adult satellite cells and embryonic muscle progenitors have distinct genetic requirements. Nature *460*, 627-631.

Miniou, P., Tiziano, D., Frugier, T., Roblot, N., Le Meur, M., and Melki, J. (1999). Gene targeting restricted to mouse striated muscle lineage. Nucleic acids research *27*, e27.

Moisescu, D.G., and Thieleczek, R. (1978). Calcium and strontium concentration changes within skinned muscle preparations following a change in the external bathing solution. J Physiol *275*, 241-262.

Prado, L.G., Makarenko, I., Andresen, C., Kruger, M., Opitz, C.A., and Linke, W.A. (2005). Isoform diversity of giant proteins in relation to passive and active contractile properties of rabbit skeletal muscles. J Gen Physiol *126*, 461-480.

Saeed, A.I., Sharov, V., White, J., Li, J., Liang, W., Bhagabati, N., Braisted, J., Klapa, M., Currier, T., Thiagarajan, M.*, et al.* (2003). TM4: a free, open-source system for microarray data management and analysis. Biotechniques *34*, 374-378.

Sakai, H., Sato, T., Kanagawa, M., Fukada, S., and Imai, Y. (2020). Androgen receptor in satellite cells is not essential for muscle regenerations. Experimental Results *1*, e21.

Sakakibara, I., Wurmser, M., Dos Santos, M., Santolini, M., Ducommun, S., Davaze, R., Guernec, A., Sakamoto, K., and Maire, P. (2016). Six1 homeoprotein drives myofiber type IIA specialization in soleus muscle. Skeletal muscle *6*, 30.

Watanabe, D., and Wada, M. (2016). Predominant cause of prolonged low-frequency force depression changes during recovery after in situ fatiguing stimulation of rat fast-twitch muscle. Am J Physiol Regul Integr Comp Physiol *311*, R919-R929.

Yamada, T., Ashida, Y., Tatebayashi, D., and Himori, K. (2019). Myofibrillar function differs markedly between denervated and dexamethasone-treated rat skeletal muscles: Role of mechanical load. PLoS One *14*, e0223551.